Microstructural Investigations on Hydrated High-Performance Cements Based on Calcium Sulfoaluminate

F. Canonico[2], G. Bernardo[1], L. Buzzi[2], M. Paris[2],
A. Telesca[1], G.L. Valenti[1],
[1]*University of Basilicata, Potenza, Italy;*
[2]*Buzzi Unicem S. p. A., Casale Monferrato, Italy*

1. INTRODUCTION

Rapid-hardening and dimensionally stable calcium sulfoaluminate (CSA) cements, first conceived by the China Building Materials Academy about 30 years ago, are very interesting binders inasmuch as they can couple engineering properties useful for structural applications with environmentally friendly characteristics of their manufacturing cycle such as low synthesis temperature and limestone requirement as well as reduced thermal input to the kiln and CO_2 generation [1-8].

During the hydration of these cements, their basic component, $C_4A_3\overline{S}$, combines with calcium sulfate to give, besides aluminium hydroxide, well developed prismatic crystals of non expansive ettringite, according to the reaction:

$$\underset{610}{C_4A_3\overline{S}} + \underset{136}{2C\overline{S}} + \underset{18}{38H} \Rightarrow \underset{1254}{C_6A\overline{S}_3H_{32}} + \underset{156}{2AH_3} \qquad \text{(I)}$$

in which each number under the compound formula indicates its molecular weight.

The most relevant features of the $C_4A_3\overline{S}$ hydration process are the following: a) the products formation rate is high; b) the reaction stoichiometry dictates the hydration mechanism [9]; c) the full formation of ettringite and aluminium hydroxide requires an elevated water amount (stoichiometric water/solid mass ratio equal to 0.78). Owing to a) and b), a peculiar state is rapidly established with stable hydration products, potentially useful for the durability of hardened cement. Owing to c), the subsequent phenomena are observed: 1) an early stopping of the hydration inasmuch as water is quickly used up for the products formation; 2) a reduced capillary porosity due to the free water consumption; 3) a persistence of anhydrous phases stable like their hydration products; 4) an environment without moisture which is fast established due to the self-drying process.

The microstructure and the technical behaviour of CSA cements hydrated according to the reaction (I) are therefore completely different from those shown by ordinary Portland cements (OPC). The OPC binding action mainly depends on calcium silicate hydrates, with variable composition and structure, consisting of multi-layers particles able to retain water molecules both on the inside and into the external voids. This situation implies a considerable sensitivity of hydrated OPC to drying-shrinkage and creep [10-11]. Moreover, the persistent free

water and the related capillary porosity, which considerably influence the engineering properties of hydrated OPC (requiring a gauging water content much higher than the stoichiometric amount), play a very limited role in regulating the hydraulic behaviour of CSA cements.
In recent years, papers concerning both the study of high-performance CSA cements and the evaluation of their technical characteristics have been published [12-17]: their good behaviour in terms of mechanical strength and durability has been emphasized. This paper is aimed at investigating the microstructure of CSA cement, paste hydrated with different water/solid mass ratios at various curing times, by means of XRD, DTA-TGA, SEM and mercury porosimetry analyses.

2. EXPERIMENTAL

2.1 Materials and properties

CSA cement was obtained from a sulfoaluminate clinker produced in a rotary kiln at about 1350°C, using limestone, bauxite and gypsum as raw materials. Its Blaine fineness was 4830 cm^2/g. The chemical and mineralogical composition, respectively evaluated by XRF and XRD analysis, is listed in Table 1. Calcium sulfates were present under both anhydrous and hydrated form, respectively belonging or added to the clinker.

Table 1- Chemical (major oxides) and mineralogical (major phases) composition of CSA cement, mass percent.

Chemical		Mineralogical	
CaO	42.5	$C_4A_3\overline{S}$	43
Al_2O_3	26.5	**Calcium sulfates (as $CaSO_4$)**	21
SO_3	19.3	**β-C_2S**	12
SiO_2	6.3	$C_5S_2\overline{S}$	8
Fe_2O_3	2.5	**C_3A**	8
MgO	1.3	**C_4AF**	4
TiO_2	0.8	**CT**	2
Na_2O	0.6		
K_2O	0.1		

Table 2 indicates some physical and mechanical properties of CSA cement together with those of an OPC (class 52.5 R) employed as a reference term. A set retarder was used for CSA cement hydration. For concrete tests on both cements, an equal amount of plasticizer was utilized. The CSA and OPC concrete composition (kg/m^3) was: cement, 400.0; water, 160 .0; plasticizer, 4.3; sand, 730.0; medium size (5-15 mm) aggregates, 460.0; large size (10-25 mm) aggregates, 650.0.
Compared with OPC, CSA cement showed less workability, much faster hardening, much lower shrinkage and permeability. Furthermore

preliminary tests on chemical (against sulfate attack) and corrosion resistance were very promising [18].

Table 2- Physical and mechanical properties of CSA and OPC cements.

	CSA						OPC					
Compressive strength on mortar, MPa[(1)]	(3h) 6.1	(8h) 23.9		(1d) 33.1	(7d) 57.7	(28d) 63.4	(3h) -	(8h) 4.6		(1d) 23.3	(7d) 41.5	(28d) 54.2
Compressive strength on concrete, MPa[(2)]	(5h) 9.0	(2d) 36.1		(7d) 44.6	(28d) 51.6	(90d) 52.5	(5h) -	(2d) 35.3		(7d) 41.5	(28d) 43.9	(90d) 42.1
Shrinkage on mortar, m/m [(3)]	(1d) 187	(7d) 281	(14d) 359	(28d) 406	(60d) 484	(90d) 578	(1d) 219	(7d) 594	(14d) 719	(28d) 875	(60d) 1047	(90d) 1234
Shrinkage on concrete, m/m [(4)]	(7d) 188		(14d) 250	(28d) 322	(60d) 368	(90d) 411	(7d) 455		(14d) 721	(28d) 785	(60d) 801	(90d) 858
Concrete slump, cm[(5)]	110						150					
Water permeability on concrete (depth of penetration), mmH_2O[(6)]	12						26					

[(1)] According to the European Standard EN 197-1
[(2)] According to the European Standard EN 12390-3
[(3)] According to the Italian Standard UNI 6687
[(4)] According to the Italian Standard UNI 6555
[(5)] According to the European Standard EN 12350-2
[(6)] According to the European Standard EN 12390-8

2.2 Samples preparation and characterization techniques

CSA cement samples were paste hydrated (water/cement mass ratios, 0.35-0.40-0.45) and investigated by XRD and DTA-TGA analyses, SEM and mercury porosimetry. The pastes, shaped as cylindrical discs (15mm high, 30mm in diameter), were cured in a FALC WBMD24 thermostatic bath at 20°C for times ranging from 3 hours to 1 year. At the end of each aging period, the discs were in part submitted to mercury porosimetry, in part broken for SEM observations or pulverized for XRD and DTA-TGA analyses after grinding under acetone (to stop hydration), followed by treating with diethyl–ether (to remove water) and storing in a desiccator over silica gel-soda lime (to ensure protection against H_2O and CO_2).

XRD analysis was performed for both qualitative and quantitative purposes (Rietveld method [19-20]), using a BRUKER-D4 XRD apparatus (equipped with a SOLEX detector) as well as EVA and TOPAS 2.1 (BRUKER) softwares for the spectra evaluation and the Rietveld determination, respectively. XRD patterns were obtained in the range 5°-55° 2θ, at the scanning rate of 0.02 2θ/sec. An automatic sample preparation machine (APM – POLYSIUS) was employed [21], using sucrose as a grinding aid; grinding time was 30 seconds. The mineralogical details of the phases used for the Rietveld determination are listed in Table 3.

DTA-TGA was carried out through a NETZSCH TASC 414/3 apparatus, operating between 20° and 1000°C with a heating rate of 10°C/min.

For SEM observations a PHILIPS XL-30 ESEM instrument was used. Specimens were metallized with gold by means of an EMITECH K 950 apparatus.
Porosity measurements were performed with a THERMO FINNIGAN PASCAL 240 Series porosimeter (maximum pressure, 200 MPa; resolution 0.01 MPa up to 100 MPa and 0.1 MPa up to 200 MPa) equipped with a low-pressure unit (140 Series) able to generate a high vacuum level (10 Pa) and operate between 100 and 400 kPa.

Table 3- Crystallographic data for phases involved in the XRD quantitative analysis.

	space group	cell length (a)	cell length (b)	cell length (c)	angle (beta)
$C_4A_3\overline{S}$ **Calcium sulfoaluminate**	Pcc2	13.01	13.04	9.16	
$C_5S_2\overline{S}$ **Ternesite**	Pcmn	10.20	15.40	6.85	
C_3A Tricalcium aluminate	Pa3	15.27			
C_4AF Brownmillerite	Pnma	5.37	14.75	5.65	
β-C_2S Larnite	$P12_1/n1$	5.51	6.76	9.29	93.96
$C\overline{S}$ **Anhydrite**	Cmcm	6.99	6.24	7.00	
$C\overline{S}H_2$ **Gypsum**	I12/a1	6.45	15.18	5.75	118.40
AH_3 Gibbsite	$P12_1/n1$	8.62	5.09	9.75	94.65
$C_6A\overline{S}_3H_{32}$ **Ettringite**	P31c	11.22		21.48	

3. RESULTS AND DISCUSSION

3.1 XRD results

During the hydration, the peak-intensities of $C_4A_3\overline{S}$ and calcium sulfates rapidly decrease while those of the other cement compounds are almost unchanged. Correspondingly, ettringite and aluminium hydroxide are the only observed hydration products.

The high consumption rate of $C_4A_3\overline{S}$ and calcium sulfates (expressed as SO_3), associated with the quick formation of ettringite and $Al(OH)_3$, can be clearly seen from Figs. 1 and 2, where the phase concentrations of reactants and products are respectively reported as a function of curing time and water/cement ratio.

Within a relatively short aging period the reactants and ettringite concentration decreases and increases, respectively, up almost stationary values. As far as $Al(OH)_3$ is concerned, the XRD peak

intensity first increases, then seems stable and at longer ages increases again.

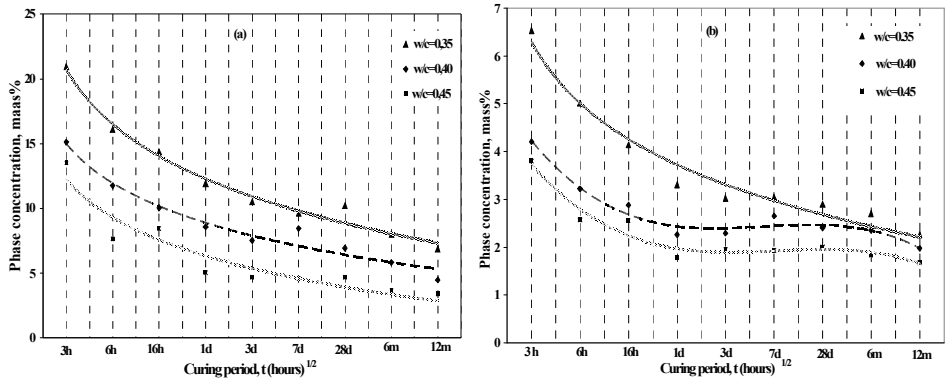

Fig.1- Consumption rate of reactants: (a) $C_4A_3\bar{S}$; (b) SO_3.

The last phenomenon is most likely due to an acquisition of crystallinity by some alumina gel. So the final increase of $Al(OH)_3$ concentration is only apparent.

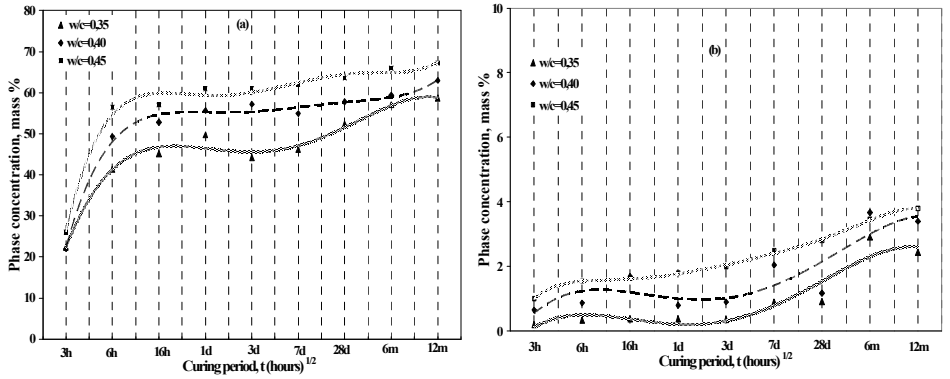

Fig.2- Formation rate of products: (a) ettringite; (b) aluminium hydroxide.

The hydration degree remarkably increases as water/cement ratio increases. In the curing period 3 hours-1 year, $C_4A_3\bar{S}$ conversion degrees comprised between 0.41 and 0.77, 0.55 and 0.85, 0.60 and 0.88 are obtained with water/cement ratios of 0.35, 0.40 and 0.45, respectively. In terms of water/$C_4A_3\bar{S} + C\bar{S}$ ratios, the values of 0.35, 0.40 and 0.45 correspond to 0.53, 0.61 and 0.68, respectively; these last figures are all lower than the stoichiometric water/reactant solids ratio for the reaction (I). This lack of water explains why: a) phases less reactive than $C_4A_3\bar{S}$ are not involved in the hydration process; b) unreacted $C_4A_3\bar{S}$ and calcium sulfates are present in the hydrated

systems even after long curing times; c) w/c ratio has a strong influence on the hydration rate.

3.2 DTA-TGA results

Thermal analysis was used in this investigation to detect ettringite and aluminium hydroxide through the DTA endothermal peaks (at about 160°-170°C and 270°-280°C, respectively) as well as the related TGA weight losses. Furthermore, TGA was utilized for the evaluation of the water content bound in the paste, useful for the calculation of the above mentioned conversion degrees. Thermal data are generally consistent with the XRD results: typical thermograms for CSA cement pastes, cured at various aging times, are shown in Fig.3.

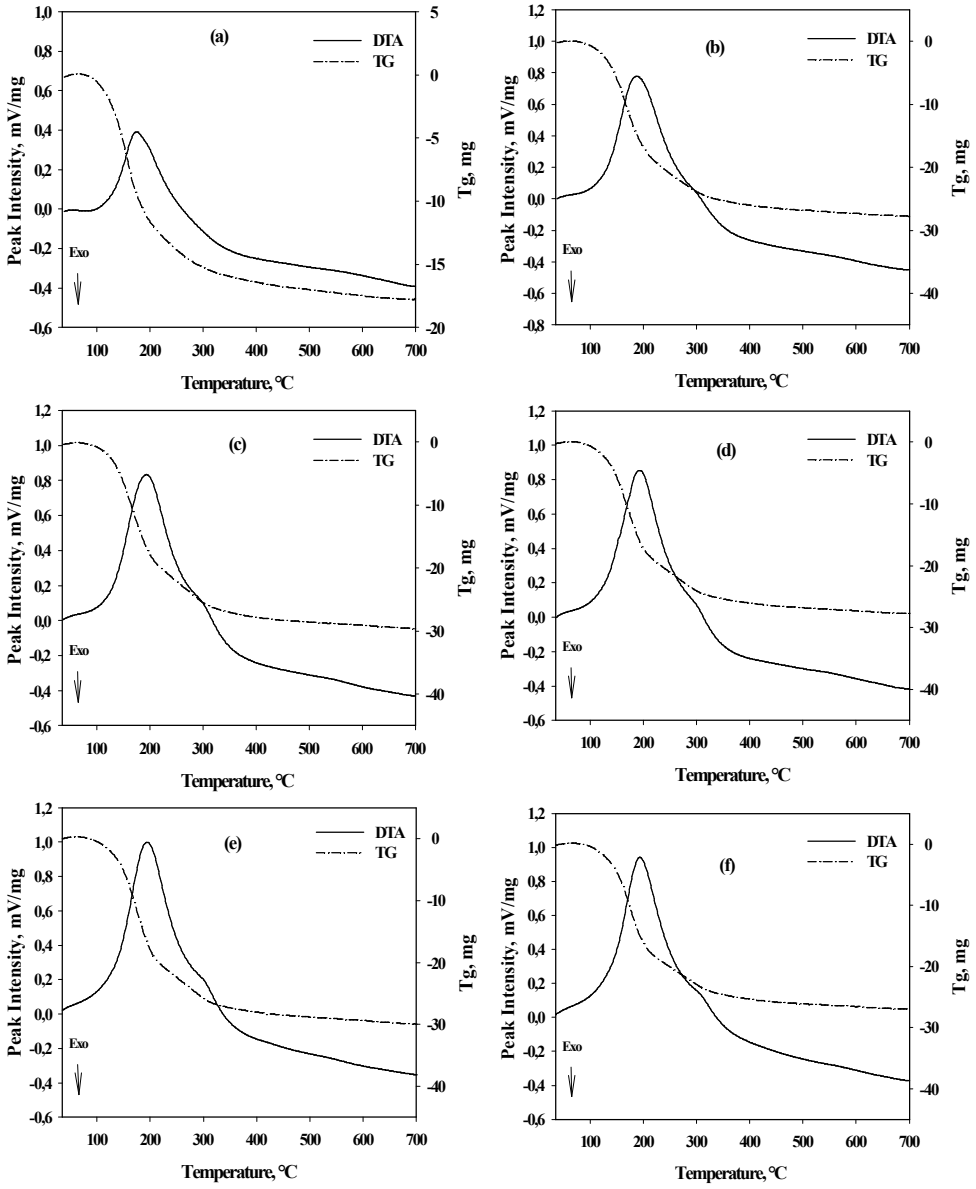

Fig.3- DTA-TGA thermograms for CSA cement paste cured at: (a) 3h; (b)1d; (c) 3d; (d) 7d; (e) 2m and (f) 9m, w/c= 0.45.

It can be noted that the signals concerning $Al(OH)_3$ are almost constant at longer ages, indicating that the related concentrations are stable.

3.3 SEM observations

The clearest images are obtained at early curing times. Fig.4 shows micrographs of CSA cement pastes (w/c=0.45) cured at 3 hours, 8 hours and 3 days. The fast rate of ettringite formation can be easily observed. Its particles already form at 3h, when the surfaces of the anhydrous grains appear corrugated, then (8h) develop as prismatic crystals having an hexagonal cross section and finally (3d) become dominant.

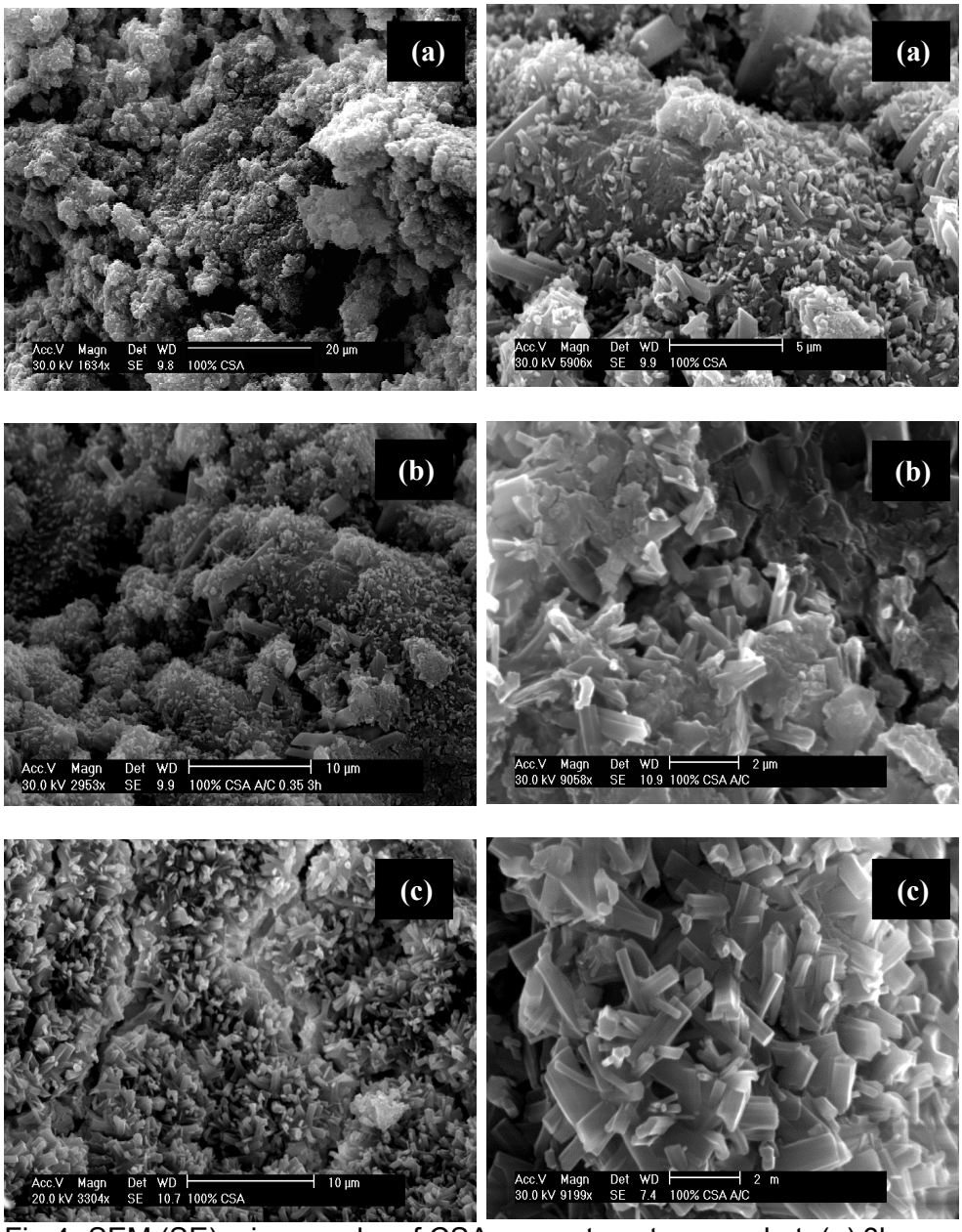

Fig.4- SEM (SE) micrographs of CSA cement pastes cured at: (a) 3h; (b) 8h; (c) 3d, w/c= 0.45 (lower magnitude on the left side).

3.4 Porosimetric results

For each sample, two plots can be obtained from the porosimetric analysis: a) cumulative and b) derivative Hg intruded volume vs. pore radius. With increasing pressure, mercury gradually penetrates the bulk sample volume. If the pore system is composed by an interconnected network of capillary pores in communication with the outside of the sample, mercury enters at a pressure value corresponding to the smallest pore neck. If the pore system is discontinuous, mercury may penetrate the sample volume if its pressure is sufficient to break through pore walls. In any case, the pore width related to the highest rate of mercury intrusion per change in pressure is known as the "critical" or "threshold" pore width. Unimodal, bimodal or multimodal distribution of pore sizes can be obtained, depending on the occurrence of one, two or more peaks, respectively, in the derivative volume plot.

As far as Portland cement hydration is concerned, the evolution of the porosimetric curves as a function of curing time and water/cement ratio is well assessed [22-26]. At early ages, the derivative plot exhibits one sharp peak, indicating a unimodal distribution of pore sizes. Later, a second more rounded peak appears at smaller pore sizes (bimodal distribution) and the first peak is shifted to the region of lower porosity, showing a reduced intensity. A similar effect, but more remarkable, is obtained, the curing time being the same, decreasing the water/cement ratio. At very low w/c ratios or quite long aging periods, the first peak disappears and the pore size distribution is unimodal. When both peaks are present, the first threshold pore width is comprised between about 2000 and 200 nanometres, depending on curing time and water/cement ratio, whereas the second one varies in a limited range, 20-60 nanometers [25]: the first peak is related to the lowest size of pore necks connecting a continuous system consisting of a network of capillary pores; the second peak corresponds to the pressure required to break through the blockages formed by the hydration products.

CSA cements pastes cured at w/c ratios of 0.35, 0.40 and 0.45 have similar porosimetric characteristics (Fig. 5) which are completely different from those of OPC. The pore size distribution is bimodal at early ages, becoming unimodal and stationary at 28 days of curing. In the bimodal distribution the region of smaller pores prevail over that related to an interconnected capillary network, except for the shortest aging time (6 hours), at which the highest values of the first and second threshold pore width are observed (191 and 31 nanometers, respectively, for w/c= 0.45). With the increase of curing time, both first and second peak shift to lower pore radii and decrease in intensity.

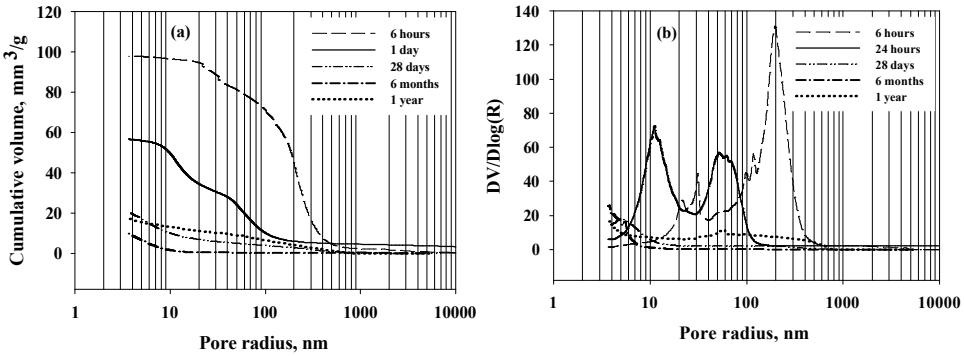

Fig.5- Intruded Hg volume vs. pore radius for CSA cement pastes cured at various ages (w/c ratio, 0.45): (a) cumulative plot; (b) derivative plot.

These data are consistent with the characteristics of the CSA cement hydration pointed out by XRD, DTA-TGA and SEM analyses. The hydration products, generated in a large amount at early curing times, are able to reduce and isolate the interior space. At longer aging periods, the evolution of porosity proceeds very slowly because hydration is almost stopped.

Taking into account the strict relationship between the permeability degree and the first threshold pore width [27], the porosimetric behaviour of CSA cements shows that they are able to develop rapidly a high impermeability and to exploit, due to the considerable isolation from the external environment, their properties useful for durability.

The porosimetric curves, in terms of total Hg intruded vo lume and preferred pore width (first threshold pore radius at 6h, second threshold pore radius later) as a function of curing time, for all the experienced w/c ratios, are described in Fig.6.

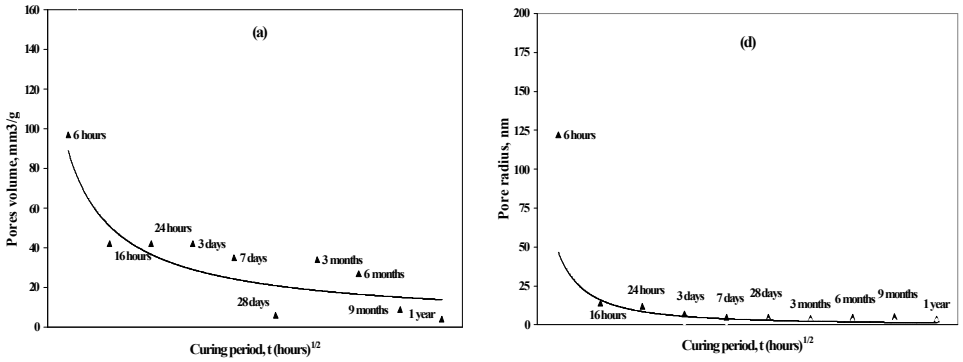

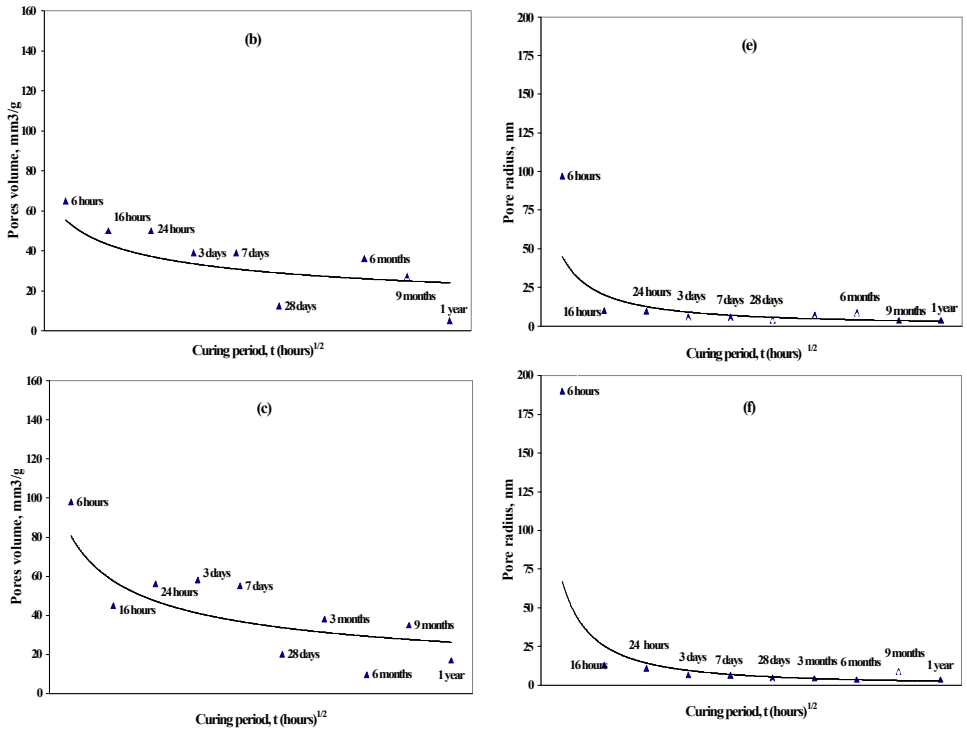

Fig.6- Total Hg intruded volume (a, b, c) and preferred pore radius (d, e, f) for CSA cement pastes vs. curing time: (a) and (d), w/c=0.35; (b) and (e), w/c=0.40; (c) and (f), w/c=0.45.

It is clearly observed a decreasing trend, particularly remarkable within the first 24 hours of hydration.

4. CONCLUSIONS

Microstructural investigations, by means of XRD, DTA-TGA, SEM and mercury porosimetry analyses, on a paste hydrated high-performance calcium sulfoaluminate (CSA) cement cured from 3 hours to 1 year at water/cement ratios equal to 0.35, 0.40 and 0.45, allow to draw the following conclusions.

1- The reaction rate of $C_4A_3\bar{S}$ with calcium sulfate and water is very high at the beginning, then rapidly declines in a few days: $C_4A_3\bar{S}$ conversion degrees of 0.41-0.60 and 0.77-0.88 were obtained at 3 hours and 1 year, respectively.

2- The hydration degree increases as water/cement ratio increases.

3- Mineralogical constituents of CSA cement such as C_3A, C_2S, C_4AF and $C_5S_2\bar{S}$, being less reactive than $C_4A_3\bar{S}$, are not involved in the reaction, inasmuch as H_2O is consumed only in the hydration of $C_4A_3\bar{S}$ and calcium sulfate. This reaction requires, for the full formation of the products (ettringite and aluminium hydroxide) a high (0.78) stoichiometric mass ratio between water and reactant solids, which is greater than those

actually used (0.53, 0.61 and 0.68, corresponding to w/c ratios of 0.35, 0.40 and 0.45, respectively).

4- The phases present in the hydrated systems are stable, except for the transition of some alumina gel to crystalline $Al(OH)_3$ after a few months of curing.

5- The porosimetric data are consistent with the results of XRD, DTA-TGA and SEM analyses. In particular, the development of the pore structure is initially very fast and a prevailing region of lower porosity is rapidly established, due to the blockages of the hydration products.

The early impermeability of hardened cement, related to the high reaction rate and the peculiar pore size distribution, enables the exploitation of useful characteristics for durability associated with the dry internal environment and the phase stability.

5. REFERENCES

[1] P.K. Mehta, Investigations on energy-saving cements, World Cem Technol 11 (4), 1980, 166-177.

[2] J. Beretka, L. Santoro, N. Sherman, G.L. Valenti, Synthesis and properties of low energy cements based on $C_4A_3\bar{S}$, Proc. 9th Int. Congr Chem Cem, New Delhi, India, 1992, vol. III, pp.195-200.

[3] J. Beretka, B. de Vito, L. Santoro, N. Sherman, G.L. Valenti, Hydraulic behaviour of calcium sulphoaluminate-based cements derived from industrial process wastes, Cem Concr Res 23, 1993, 1205-1214.

[4] J. Majling, S. Sahu, M.Vlna, Della M. Roy, Relationship between raw mixture and mineralogical composition of sulphoaluminate belite clinkers in the system $CaO-SiO_2-Al_2O_3-Fe_2O_3-SO_3$, Cem Concr Res 23, 1993, 1351-1356.

[5] G. Belz, J. Beretka, M. Marroccoli, L. Santoro, N. Sherman, G.L. Valenti, Use of fly ash, blast furnace slag and chemical gypsum for the synthesis of calcium sulphoaluminate based cements, Proc 5th CANMET/ACI Int. Conf. on Fly Ash, Silica Fume, Slag and Natural Pozzolans in Concrete, Milwaukee, USA, 1995, SP-153, 1995, vol. 1, pp.513-530.

[6] J. Beretka, R. Cioffi, M. Marroccoli, G.L. Valenti, Energy-saving cements obtained from chemical gypsum and other industrial wastes, Waste Management 16, 1996, 231-235.

[7] G. Bernardo, M. Marroccoli, F. Montagnaro, G.L. Valenti, Use of fluidized bed combustion wastes for the synthesis of low energy cements, Proc. 11th Int Congr Chem Cem, Durban, South Africa, 2003, vol. 3, pp. 1227-1236.

[8] E. Gartner, Industrially interesting approaches to ''low-CO_2'' cements, Cem Concr Res 34, 2004, 1489-1498.

[9] F. Hanic, I. Kapralik and A. Gabrisova, Mechanism hydration reactions in the system $C_4A_3\bar{S}$ -CS-CaO-H_2O referred to hydration of sulphoaluminate cements, Cem Concr Res 19, 1989, 671-682.

[10] P. K. Mehta, Hardened cement paste – Microstructure and its relationship to properties, Proc. 8th Int Congr Chem Cem, Rio de Janeiro, Brazil, 1986, vol. 1, 113-121.

[11] R. E. Oberholster, Pore structure, permeability and diffusivity of hardened cement paste and concrete in relation to durability: status and prospects, Proc. 8th Int Congr Chem Cem, Rio de Janeiro, Brazil, 1986, vol. 1, 323-335.
[12] Muzhen Su, Yanmou Wang, Liang Zhang, Dedong Li, Preliminary study on the durability of sulfo/ferro-aluminate cements", Proc. 10th Int Congr Chem Cem, Goteborg, Sweden, 1997, vol. 4, pp. 4iv029 (12 pp.).
[13] Wang Lan, F.P. Glasser, Hydration of calcium sulphoaluminate cements, Adv Cem Res, 8 (31), 1996, 127-134.
[14] L. Zhang, F.P. Glasser, New concretes based on calcium sulphoaluminate cements, in: R.k. Dhir, D. Dyer (Eds), Modern Concrete Materials, Thomas Telford, London, 1999, pp. 261-274.
[15] F.P. Glasser, L. Zhang, High-performance cement matrices based on calcium sulphoaluminate-belite compositions, Cem Concr Res 31, 2001, 1881-1886.
[16] F.P. Glasser, Advances in sulphoaluminate cements, Proceedings of the 5th International Symposium on the Cement and Concrete, Shanghai, China, 2002, vol. 1, pp. 14-24.
[17] G. Bernardo, A. Telesca, G. L. Valenti, A porosimetric study of calcium sulfoaluminate cement pastes cured at early ages, Cem Concr Res 36, 2006, 1042-1047.
[18] BUZZI-UNICEM Labs. Internal Reports (unpublished results).
[19] HM Rietveld, A profile refinement method for nuclear and magnetic structures, J Appl Cryst, 2, 1969, pp 65-71.
[20] D.L. Bish, S.A. Howard, Quantitative analysis using Rietveld method. J Appl Cryst, 21, 1988, pp. 86-91.
[21] M.Enders, Quantitative XRD-Analysis in automated cement laboratories: requirement for the sample preparation. ZKG International 5, 2003, pp 54- 62.
[22] A. Bentur, The pore structure of hydrated cementitious compounds of different chemical composition, J Amer Cer Soc 63 (7-8), 1980, 381-386.
[23] E.J. Garboczi, Permeability, diffusivity, and microstructural parameters: A critical review, Cem Concr Res 20, 1990, 591-601.
[24] N. Hearn, R.D. Hooton, Sample mass and dimension effects on mercury intrusion porosimetry results, Cem Concr Res 22, 1992, 970-980.
[25] R.A. Cook, K.C. Hover, Mercury porosimetry of hardened cement pastes, Cem Concr Res 29, 1999, 933-943.
[26] S. Diamond, Mercury porosimetry – An inappropriate method for the measurement of pore size distributions in cement-based materials, Cem Concr Res 30, 2000, 1517-1525.
[27] B.k. Nyame J.M. Illston, Capillary pore structure and permeability of hardened cement paste, Proc. 7th Int Congr Chem Cem, Paris, France, 2003, vol. 4, pp. VI/181-VI/185.